

# PARTICLE IMAGE IDENTIFICATION, CLASSIFICATION AND CORRECTION TECHNIQUES IN DIGITAL HOLOGRAPHIC MICROSCOPY

## KHAIRUL FIKRI BIN TAMRIN



05-4506832 Vestaka.upsi.edu.my

### A THESIS SUBMITTED IN PARTIAL FULFILMENT OF THE REQUIREMENTS FOR THE DEGREE OF DOCTOR OF PHILOSOPHY

## FACULTY OF ARTS, COMPUTING AND CREATIVE INDUSTRY UNIVERSITI PENDIDIKAN SULTAN IDRIS

2016





Perpustakaan Tuanku Bainun Kampus Sultan Abdul Jalil Shah PustakaTBainun

ptbupsi

iv

#### ABSTRACT

This thesis aimed to investigate digital methods for identification, classification, and correction of particle images using digital holographic microscopy. The work begins with a micro-scale flow experiment employing a digital off-axis holographic microscope. To overcome noise from out-of-focus particle images due to the increase in the particle concentration, a new particle image identification algorithm with threedimensional reconstruction was introduced. It shows that individual particle images could be identified at about 62% of the expected number of particles. However, a cylindrical micro-channel used in the experiment was found as the main source of astignatism. Following this, an automatic image classification using neural network was proposed to classify reliable and astigmatic particle images. A feed-forward backpropagation neural network with two class classifier was trained, achieving overall accuracy of 99.8%. Next, an original method of aberration correction using a priori information and digital wavefront aberration processing was applied. Astigmatism introduced by the micro-channel was modelled according to quadratic C os phase function and optimized using peak detection algorithm. The results show that astigmatism in the detected particle images was effectively compensated. A variant digital off-axis holographic microscope was later developed for large-scale flow measurement, allowing for the first time both amplitude and phase of the holographically reconstructed images to be registered simultaneously. The aberration introduced by a tilt in the optical hologram during the reconstruction was effectively corrected using adaptive optics. In overall, the work discussed in the thesis has proven effective to overcome noise and aberration. The main implication is that the holographic techniques can be successfully employed in complex three-dimensional fluid flow measurements.





pustaka.upsi.edu.my

Perpustakaan Tuanku Bainun Kampus Sultan Abdul Jalil Shah

PustakaTBainu

ptbupsi

V

#### TEKNIK MENGENALPASTI, MENGKLASIFIKASI DAN MEMPERBAIKI IMEJ ZARAH DALAM MIKROSKOP HOLOGRAFI DIGITAL

#### ABSTRAK

Kajian ini bertujuan untuk menyiasat pelbagai teknik digital menggunakan mikroskop holografi untuk proses mengenalpasti, mengklasifikasi, dan membaiki imej zarahzarah bagi mengatasi masalah hingar dan aberasi. Kajian ini bermula dengan menjalankan eksperimen berskala kecil menggunakan mikroskop holografi digital. Untuk mengatasi masalah hingar yang berpunca oleh imej zarah-zarah yang tidak fokus, satu teknik pengenalpastian imej telah disyorkan. Hasilnya, sebanyak 62% imej zarah-zarah berjaya dikenal pasti. Eksperimen ini mendapati penggunaan kolong saluran mikro merupakan punca utama astigmatisma. Klasifikasi imej secara otomatik menggunakan rangkaian neural disyorkan untuk mengklasifikasi imej zarah-zarah 05 yang bagus dan yang dipengaruhi oleh astigmatisma. Klasifikasi imej dua kelas berdasarkan rangkaian neural feed-forward backpropagation telah dilatih dan hasilnya mampu untuk mengenalpasti imej pada kadar ketepatan 99.8%. Satu kaedah telah dihasilkan untuk mengatasi masalah astigmatisma dengan menggunakan pemprosesan aberasi digital dan informasi priori. Astigmatisma yang wujud akibat penggunaan kolong saluran mikro telah dimodelkan berdasarkan fungsi fasa kuadratik dan dioptimumkan menerusi algoritma pengesanan puncak. Astigmatisma yang terkandung dalam imej zarah-zarah berjaya diperbetulkan. Sebuah mikroskop holografi digital yang tidak berpaksi telah dibina untuk eksperimen berskala besar. Untuk pertama kalinya, kedua-dua amplitud dan fasa yang terhasil daripada proses rekonstruksi imej secara holografi berjaya direkodkan serentak. Imej zarah-zarah yang direkodkan menggunakan filem hologram didapati dipengaruhi oleh aberasi yang berpunca akibat kedudukan hologram yang serong. Aberasi tersebut berjaya diperbetulkan menggunakan optikal adaptasi. Secara keseluruhannya, teknik-teknik digital yang telah disyorkan di dalam tesis ini telah terbukti efektif untuk mengatasi masalah hingar dan aberasi. Implikasinya, teknik-teknik holografi ini mampu menjayakan pengukuran bendalir kompleks yang bersifat tiga dimensi.





## **TABLE OF CONTENTS**

				Page			
	DECLARATI	ON OF	ORIGINAL WORK	ii			
	ACKNOWLEDGEMENTS						
	ABSTRACT						
	ABSTRAK						
	TABLE OF C	ONTEN	NTS	vi			
	LIST OF TAB	LES		xi			
0	LIST OF FIGU	taka.upsi.o	edu.my Perpustakaan Tuanku Bainun Kampus Sultan Abdul Jalil Shah DustakaTBainun	tbupsi xviii			
	LIST OF APPENDICES CHAPTER 1 INTRODUCTION						
		1.1	Introduction and Research Background	1			
		1.2	Problem Statement	3			
		1.3	Research Objectives	6			
		1.4	Research Scope	6			
		1.5	Thesis Outline	8			
	CHAPTER 2 LITERATURE REVIEW						
		2.1	Introduction	10			
		2.2	Basic Holographic Recording and Reconstruction Setups	13			



vii

05-4506832	pus	taka.upsi.e		Perpustakaan Tuanku Bainun Kampus Sultan Abdul Jalil Shah PustakaTBainun	ptbupsi
		2.3		Development of Holographic Particle Image imetry (HPIV)	22
			2.3.1	Forward-scatter In-line Holography	22
			2.3.2	Forward-scatter Off-axis Holography	26
			2.3.3	Side-scatter Off-axis Holography	34
			2.3.4	Back-scatter Off-axis Holography	36
			2.3.5	Application of Bacteriorhodopson Film in HPIV	40
		2.4	Comp	arison of HPIV Techniques	41
		2.5	Transi	tion from Film-based to Digital Holography	45
		2.6	Digita	l Holographic Microscopy	47
		2.7	Digita	l Holographic Particle Image Velocimetry	50
			2.7.1	Noise Suppression	50
05-4506832	pus	taka.upsi.e	2.7,2	Correction of Aberrations PustakaTBainun	ptbup53
			2.73	Particle Image Identification	54
		2.8	Summ	ary	60
CHAP'	FER 3	DIME	ENSIO	MENTAL INVESTIGATION OF THREI NAL PARTICLE AGGREGATION USIN OLOGRAPHIC MICROSCOPY	
		3.1	Introd	uction	61
		3.2	Digita	l Holographic Microscopy	67
			3.2.1	Digital Holographic Recording	67
			3.2.2	Digital Holographic Reconstruction	73
		3.3	Metho	odology	77
			3.3.1	Experimental Setup	77
			3.3.2	Preliminary Experiment	81
			3.3.3	Experiments	84
05-4506832	pus	taka.upsi.e	edu.my	Perpustakaan Tuanku Bainun Kampus Sultan Abdul Jalil Shah PustakaTBainun	ptbupsi

	•	٠	٠
V		1	1

05-4506832	pustaka.upsi.e	du.my f Perpustakaan Tuanku Bainun Kampus Sultan Abdul Jalil Shah 🛛 💭 PustakaTBainun	ptbupsi
	3.4	A New Particle Image Identification Technique	86
	3.5	Results	96
	3.6	Summary	99
CHAPTER	HOLO	TICLE IMAGE CLASSIFICATION IN DIGITAL DGRAPHIC MICROSCOPY USING NEURAL VORK	
	4.1	Introduction	101
	4.2	Classification of Particle Images	107
		4.2.1 Feed-forward Backpropagation Neural Network	107
	4.3	Data Pre-processing	109
	4.4	Performance Analysis	113
		4.4.1 Mean Squared Error	113
<u>_</u>		4.4.2 Confusion Matrix	114
05-4506832	pustaka.upsi.e	4.4.3 Perpustakaan Tuanku Bainun Kampus Sultan Abdul Jalil Shah Regression Plot	ptbupsi 116
	4.5	Results	118
	4.6	Discussion	124
	4.7	Summary	124
CHAPTER	HOLO	GMATISM CORRECTION IN DIGITAL OGRAPHIC MICROSCOPY USING A PRIORI RMATION	
	5.1	Introduction	126
	5.2	Theory of Astigmatism Correction	128
	5.3	Wavefront Aberration Correction	131
	5.4	Results	134
	5.5	Discussion	137
	5.6	Summary	138

ix

05-4506832 🔮 pus	staka.upsi.	edu.my f Perpustakaan Tuanku Bainun Kampus Sultan Abdul Jalil Shah 99 PustakaTBainun	ptbupsi
CHAPTER 6	HOL PAR	ELOPMENT OF A NOVEL OFF-AXIS DIGITA OGRAPHIC MICROSCOPE IN HOLOGRAPH FICLE IMAGE VELOCIMETRY FOR LARGE W MEASUREMENT	IC
	6.1	Introduction	140
	6.2	Holographic Recording	142
		6.2.1 Path Length Compensation	145
		6.2.2 Noise Suppression	145
	6.3	Holographic Reconstruction and a Novel Digital Holographic Microscope	146
		6.3.1 A Novel Off-axis Digital Holographic Microscope	148
	6.4	Summary	152
CHAPTER 7	PAR	RRATION CORRECTION OF HOLOGRAPHI FICLE IMAGES USING DIGITAL HOLOGRA ROSCOPY	
<b>(C)</b> 05-4506832 <b>(C)</b> pus	staka.upsi. 7.1	edu.my Perpustakaan Tuanku Bainun Introduction mpus Sultan Abdul Jalil Shah	ptbupsi 153
	7.2	Theory of Aberration Correction	158
	7.3	Experiments	162
		7.3.1 Samples	162
		7.3.2 Hologram Wet Processing	165
	7.4	Wavefront Aberration Measurement	166
	7.5	Results	171
	7.6	Discussion	175
	7.7	Summary	176
CHAPTER 8	SUM	MARY AND FUTURE WORK	
	8.1	Summary	179
	8.2	Recommendations for Future Work	183
🕓 05-4506832 🔮 pus	staka.upsi.	edu.my f Perpustakaan Tuanku Bainun Kampus Sultan Abdul Jalil Shah Ӯ PustakaTBainun	ptbupsi

05-4506832 Pustaka.upsi.edu.my 8.3 Publicati	Perpustakaan Tuanku Bainun Kampus Sultan Abdul Jalil Shah ons Arising from Thesis	PustakaTBainun	ptbupsi 185
REFERENCES			187
APPENDIX A			199
APPENDIX B			200
APPENDIX C			201





O5-4506832 V pustaka.upsi.edu.my

Х

PustakaTBainun



C

O5-4506832 Spustaka.upsi.edu.my f Perpustakaan Tuanku Bainun Kampus Sultan Abdul Jalil Shah PustakaTBainun btupsi

## LIST OF TABLES

Table		Page
2.1	Comparison of Various Types of Holographic Recording and Reconstruction Setups	21
2.2	Performance Comparison of HPIV Systems and Chronologically Tabulated in Reverse Order	43
2.3	Comparison of Information Capacity of Three Dissimilar Recording Media	47
2.4	Performance Comparison of DHPIV Systems and Chronologically Tabulated in Reverse Order	58
<b>3.1</b> 05-4506832	Blood Flow and Experimental Parameters pustaka.upsi.edu.my  F Perpustakaan Tuanku Bainun Kampus Sultan Abdul Jalil Shah  PustakaTBainun	84 ptbupsi
3.2	Mixtures and Their Zeta-potential	85
4.1	Specifications of Neural Network	112
4.2	3D Positions of the Astigmatic Particle Images Identified Using the Trained Neural Network	121
7.1	Description of Various Particles Used in the Experiment	164
7.2	Preparatory Steps for Wet Processing of the Hologram	166
7.3	Calculated Polynomial Coefficients to Estimate the Phase of the Reference Object	169
7.4	Strehl Ratio of Various Particle Sizes as a Result of Wavefront Correction	175



C

O5-4506832 Spustaka.upsi.edu.my Perpustakaan Tuanku Bainun Kampus Sultan Abdul Jalil Shah SpustakaTBainun btupsi

xii

## LIST OF FIGURES

Figure		Page
1.1	Flowchart showing the scope and outline of the present research	7
2.1	Forward-scatter in-line holographic (a) recording, and (b) reconstruction setups. NA stands for numerical aperture	12
2.2	Light scattering by a 1 $\mu$ m oil particle in air medium using a green laser (wavelength, $\lambda = 532$ nm) according to Mie's theory (Raffel et al., 1998). The intensity between two neighbouring circles is differ by a factor of 100	15
2.3 05-4506832	Light scattering by a 10 $\mu$ m oil particle in air medium using a green laser (wavelength, $\lambda = 532$ nm) according to Mie's theory (Raffel et al., 1998). The intensity between two neighbouring circles is differ by a factor of 100 <sup>-</sup> Kampus Sultan Abdul Jalil Shah	15 ptbupsi
2.4	Forward-scatter off-axis holographic (a) recording, and (b) reconstruction setups	17
2.5	Side-scatter off-axis holographic (a) recording, and (b) reconstruction setups	18
2.6	Back-scatter off-axis holographic (a) recording, and (b) reconstruction setups	19
2.7	Typical optical recording arrangement for in-line particle holography	23
2.8	Off-axis viewing of an in-line hologram (after Meng and Hussain (1991))	24
2.9	Stereo-HPIV (after Scherer and Bernal (Scherer and Bernal, 1997))	25
2.10	High-pass filtering technique in forward-scatter off-axis geometry (after F. Liu and Hussain (Liu and Hussain, 1998))	27
2.11	Optical arrangement that utilised triangular tank with a mirror to simultaneously record an object and its mirror image (after Sheng et al. (2003))	29

	٠	٠	٠	
Х	1	1	1	

2.12	Schematic diagram of a near-forward scatter off-axis setup and method used to suppress the un-diffracted object beam (after Barnhart et al. (1994))	31
2.13	Holographic recording setup utilising light sheet object beam (after Fabry (1998))	32
2.14	Use of a prism in the reconstruction geometry to produce stereoscopic pairs of particle images (after Fabry (Fabry, 1998)). The 3D particle displacement, s is determined such that $s = sqrt(s_i^2+s_2^2)$	33
2.15	Hologram recording with a tilted object beam to suppress zero- order diffraction (after Von Ellenrieder et al. (2001))	31
2.16	Employment of cylindrical light volume and alignment grid in side- scatter geometry. Planar HPIV setup employs a light sheet in place of the existing cylindrical light volume (after Lozano et al. (1999))	34
2.17	(a) Reflection geometry using converging reference waves. Use of a fabricated holographic optical element allows the second exposure to be displaced by a known displacement. (b) Object conjugate	38
05-4506832	reconstruction geometry using a fibre-optic probe as a means to recreate the original reference waves (after Barnhart et al. (2000; 2002b)). For clarity, a single particle is shown in the diagram	ptbupsi
3.1	(c) The proposed particle image identification technique attempts to overcome the main limitation of the common particle image identification as illustrated in scenarios (a) and (b).	65
3.2	(a) Digital holograhic microscope used for the experiment, and (b) schematic diagram of the experiment	69
3.3	(a) Optical geometry of a digital off-axis forward-scatter holographic microscope, and (b) Fourier transform of the interference pattern recorded on the CCD plane	70
3.4	The Ewald sphere of an infinitely thin spherical shell with radius, $ \mathbf{k}  = 1/\lambda$ , representing spectrum $\tilde{U}(\mathbf{k})$ . The holographic microscope measures in forward scatter and light scattering is filtered by finite NA of the objective lens or the measure of the solid angle covered by the objective. NA=0.55 refers to the solid angle subtended by the cone	76
3.5	Method to expel air	78
3.6	Image of (a) a test section, and (b) its cross-sectional view	79
05-4506832	😵 pustaka.upsi.edu.my 📔 Perpustakaan Tuanku Bainun Kampus Sultan Abdul Jalil Shah 🍞 PustakaTBainun 😈	ptbupsi

O5-4506832 Spustaka.upsi.edu.my f Perpustakaan Tuanku Bainun Kampus Sultan Abdul Jalil Shah PustakaTBainun btupsi

O5-4506832 Og pustaka.upsi.edu.my Perpustakaan Tuanku Bainun Kampus Sultan Abdul Jalil Shah

2				

3.7	Surface roughness of the inner wall of Tygon's tubing showing bulges and lumps of varying sizes using (a) 5x and (b) 40x objectives	80
3.8	Effects of background noise removal. Images are approximately 200 um (length) x 150 um (width)	81
3.9	Digital image of an interior wall of the sectioned tubing showing deposition of particles	83
3.10	Particles have the tendency to be readily dropped out of suspension and adhered to tube walls due to attraction force of opposite charges. Passivation attempts to remove the surface potential of the tubing and consequently to mitigate deposition of particles to tube walls	83
3.11	Typical image of a pair of particles that are in close proximity. The reasonable size of the circular mask used in the algorithm is 7 pixels or approximately 2.59 $\mu$ m in diameter. The mask is centred at the peak intensity. Image size is 15 $\mu$ m x 15 $\mu$ m (41 x 41 pixels).	87
3.12	Illustration of steps taken in particle image detection technique	88
3.13 05-4506832	Flowchart showing demodulation of the recorded digital hologram and particle image identification algorithm performed in MATLAB <sup>TM</sup> software	89 ptbupsi
3.14	Top figures illustrate absolute of reconstructed particle images corresponding to the first and the 1500th particles respectively. Image size is 15 $\mu$ m x 15 $\mu$ m (41 x 41 pixels). Bottom figures represent their corresponding intensity values. Note: particles are located at the centre of image	91
3.15	Typical image of a pair of particles that are in close proximity. Image size is 15 $\mu$ m x 15 $\mu$ m (41 x 41 pixels)	93
3.16	A single particle image but reported as a pair. Image size is 15 $\mu$ m x 15 $\mu$ m (41 x 41 pixels)	93
3.17	Complication of edge correction to handle boundary effect. Hatch section represents area within an increment of dr	95
3.18	Two graphs of radial distribution function, $g(r)$ versus inter-particle distance, r/um. Two graphs are presented here to compare the result of manual particle identification	96
3.19	Results from all four experiments showing the trends of radial distribution function, $g(r)$ with respect to inter-particle distance,	98

r/um



PustakaTBainun ptbupsi

PustakaTBainun

$\bigcirc$	05-4506832	
$\smile$		

12		e+	-				
.7	Pu						

Perpustakaan Tuanku Bainun Kampus Sultan Abdul Jalil Shah

```
PustakaTBainun ptbupsi
```

4.1	Cross-sectional view of the test section and refractive indices of the media	106
4.2	Block diagram for training of neural network. (b) Diagram of the neural network consisting of 121 inputs (cropped image of 11 by 11 pixels) and two outputs (Class 1, Class 2)	109
4.3	One of the original images ( $41x41$ pixels) obtained using digital holographic microscopy was cropped to smaller image size of $11x11$ pixels. Each pixel carries amplitude and phase information, and the absolute intensity is then normalized from 0 to 255. The pixel is then arranged accordingly, forming the input layer of the neural network with 121 neurons	111
4.4	The performance plot of the mean squared error (MSE) is usually used to indicate the iteration at which the validation performance reached a minimum	114
4.5	Confusion matrix: green and red shaded cells represent correct and incorrect classifications, respectively. All 1043 good samples were correctly classified as Class 1. On the other hand, five astigmatic samples were correctly classified as Class 2 while the remaining two samples were mistakenly identified as Class 1	115
05-4506832 4.6	Regression plots showing the relationship between outputs and targets for training, validation and testing data	ptbupsi 117
4.7	Astigmatic particle images with classification accuracies greater than 50% were subjected to manual inspection: (a) 55.7% (Exp4_4min no. 561) and (b) 65.3% (Exp4_32min no. 775)	119
4.8	The trained neural network falsely identified the above image as astigmatic with a reported classification accuracy of 86.4% (Exp4_16min no. 106). A footprint of the mask applied to a neighbouring particle image causes it to appear astigmatic	119
4.9	The trained neural network failed to identify the astigmatic particle images: (a) (Exp4_32min no. 293), and (b) (Exp4_8min no. 206)	120
4.10	3D distribution of astigmatic particle images within the interrogation volume. Majority of the particles are located closer to the bottom and nearer to the wall boundary i.e., further away from the central axis of the micro-channel	122
4.11	Images of astigmatic particles with classification accuracy greater than 90%. Note: Peak centroid is located at the centre of the image	123

$\bigcirc$	05-4506832	
$\smile$		

1.21	101	0			
9					

Perpustakaan Tuanku Bainun Kampus Sultan Abdul Jalil Shah

xvi

5.1	Illustration of the technique to correct for astigmatism in the reconstructed particle images	129
5.2	Outline of procedures for correcting aberration in the particle images	132
5.3	Estimated quadratic phase distribution used for correcting astigmatism in the particle images. (a) Two-dimensional and (b) three-dimensional views	133
5.4	Wrapped phase distribution of the quadratic phase function used for correcting astigmatism in the particle images	133
5.5	Left column shows astigmatic particle images having classification accuracy greater than 90%. Middle column shows the high-contrast of the same images. Right column shows the high-contrast of the same images after astigmatism correction. Note: Peak centroid is located at the centre of the image	135
6.1	Off-axis holographic recording set-up using a converging object wave with a beam stop and a plane reference wave	143
05-65.25832	Optical setup of the Continuum Inc. laser alil Shah	) ptb <b>14</b> 4
6.3	Hologram reconstruction setup and utilisation of an off-axis digital holographic microscope (DHM) to digitise both the amplitude and phase of the reconstructed particle images. A conjugate reference wave is employed to reconstruct the hologram containing particle field, and eventually the reconstructed images are digitised using the DHM	147
6.4	Schematic diagram of an off-axis digital holographic microscope probe. The magnified image of the reconstructed object and the reference wave interferes on the CCD plane with an intersecting angle, $\theta_{ccd}$ less than that of Nyquist's limit. An off-axis digital hologram of the object is finally recorded	148
6.5	An off-axis digital holographic microscope	149
6.6	Interference fringes due to reference and object beams (no object present) using the holographic microscope. Inset: magnified of fringes	150
6.7	Distribution of spectra in Fourier domain that was experimentally acquired from the holographic recording of a diffuse object using the holographic microscope	151

7.1	An off-axis holographic recording setup. The holographic plate is tilted at Brewster's angle with respect to the oncoming reference wave to minimise reflection	158
7.2	Digital image of 10 $\mu$ m polystyrene microspheres deposited on a glass cover slip and captured using a 40x objective. The image was taken against dark background so that any anomaly of the particle sphericity can be easily detected. Due to tilt of the glass cover slip, the clustered particles appear in-focus at the top region and they appear out-of-focus towards the bottom region	163
7.3	Outline of procedures for correcting aberration in the particle images	167
7.4	(a) Amplitude distribution and (b) wrapped phase of the reference object. $k_x$ and $k_y$ are wave vectors	168
7.5	Three-dimensional plot of the measured phase distribution of the reference object used to correct for the aberration in the reconstructed images of 10, 5 and 3 $\mu$ m polystyrene spheres. It shows third-order aberration characterised by astigmatism and defocus	170
05-756,832	Amplitude of the aberrated 10 $\mu$ m particle image (b) Amplitude of the corrected 10 $\mu$ m particle image. Cropped image size is 158x158 $\mu$ m <sup>2</sup>	ptb1751
7.7	Amplitude of the aberrated 5 $\mu$ m particle image (b) Amplitude of the corrected 5 $\mu$ m particle image. Cropped image size is 158x158 $\mu$ m <sup>2</sup>	172
7.8	Amplitude of the aberrated 3 $\mu$ m particle image (b) Amplitude of the corrected 3 $\mu$ m particle image. Cropped image size is 158x158 $\mu$ m <sup>2</sup>	173
8.1	Introduction of multiple guide stars inside a glass tank as a means to universally cater for different aberrations inherent in the imaging	185

O5-4506832 Sultan Abdul Jalil Shah

C.

system

ptbupsi



PustakaTBainun



C

xviii

#### NOMENCLATURE

	А	amplitude
	a <sub>0-5</sub>	scalar constants of a polynomial fit
	D	optical density
	DoF	depth-of-focus
	DHPIV	digital holographic particle image velocimetry
	DHM	digital holographic microscopy
	d	diameter of a diffraction-limited particle
	$d_{\mathrm{f}}$	distance between two consecutive interference fringes
) 0!	E 5-4506832 🔮 p	energy of a reconstructed particle image Perpustakaan Juanku Bainun Kampus Sultan Abdul Jalil Shah focal point
	$g(r_i)$	separation distance of particle pairs
	HPIV	holographic particle image velocimetry
	I(x,y)	intensity of interference pattern at the recording plane (x,y)
	I <sub>ccd</sub>	interference recorded on the CCD plane
	Io	intensity of a focussed particle image
	k	spatial frequency $(k_x, k_y, k_z)$
	L	depth volume
	MSE	mean squared error
	Ν	total number of particles
	$N_i$	number of particle pairs separated by a distance $\left(r_{i}+dr\right)$
	$N_p$	total number of correlation pairs
	NA	numerical aperture
	NIST	National Institute of Standards and Technology

	~			
-7	a 1	\		
. (	×.			-4
· \	· · · ·	/	~~	

**t**<sub>0</sub> 05-4506832  $U_0(\mathbf{r})$ 

η

4506832	pustaka.up	

f

NN	neural network
n	refractive index
n <sub>s</sub>	particle density
0	complex amplitude of the scattered field
Р	scattering power of a diffraction-limited particle
R	complex amplitude of the reference field
r	3D position vector $(r_x, r_y, r_z)$
$r_i$	inter-particle distance
SNR	signal-to-noise-ratio
s <sub>d</sub>	shadow density
Т	exposure time
t	time
t	amplitude transmittance of a hologram
$t_0$ 5-4506832 $U_0(\mathbf{r})$	constant background transmittance pustaka.upsi.edu.my 11 Kampus Sultan Abdul Jalil Shah 3D reconstruction of a complex amplitude
V	total volume of a system
(x,y)	recording plane
$(x_i,y_i,z_i)$	coordinate of a virtual image
(x <sub>0</sub> ,y <sub>0</sub> ,z <sub>0</sub> )	coordinate of a real image
$(x_R, y_R, z_R)$	coordinate of a reference field
α	sin $\alpha$ is the numerical aperture of a focussed image
β	slope of t versus E of a photographic material
γ	film gamma
λ	wavelength

- angular aperture Ω
- standard deviation of an intensity due to background noise σ
  - $\sin\eta$  is the numerical aperture of a converging beam

ptbupsi

ptbupsi

PustakaTBainun

$\sim$						
6)		5.	.4			6
	~	~		~	~	~

6832 🜍 pustaka.upsi.edu.my 🗗 Perpustakaan Tuanku Bainun Kampus Sultan Abdul Jalil Shah

PustakaTBainun ptbupsi

θ	angle of incidence
$\theta_{wedge}$	wedge angle
$\theta_{ccd}$	intersecting angle between the object and the reference fields on the CCD plane
$\Delta x$	pixel size
$\Delta V_i$	volume of a discrete shell located at r <sub>i</sub>





O5-4506832 V pustaka.upsi.edu.my

**Y** PustakaTBainun



xxi

## LIST OF APPENDICES

А	Preparation of Tyrodes Buffer	199
В	Calculation of Number of Blanks Particles (Albumin Spheres) in 1 ml Flow Volume	200
С	Calculation of Particle Number Concentration	201





O5-4506832 V pustaka.upsi.edu.my



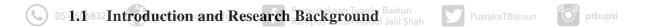


05-4506832 Vertaka.upsi.edu.my

PustakaTBainun O ptbupsi

#### **CHAPTER 1**

#### **INTRODUCTION**



Swirls, tornados and cyclones are interesting examples of turbulent flows that exist in nature. In industry, turbulence plays some important roles to increase rate of mixing and heat transfer (Pope, 2000) that in turn depend on the formation of vortices (eddies) which appear on many different length scales. On the other hand, blood flow inside the human body is by nature pulsatile and laminar, ensuring consistent delivery of vital nutrients, oxygen and antibodies throughout the system (Lima, Ishikawa, Imai, and Yamaguchi, 2012). However, the blood flow becomes turbulent when blood vessels are abnormally constricted. In general, turbulent flows are highly complex and inherently three-dimensional. In order to understand and characterise the physics which underpin various turbulent phenomena, it is important to resolve both large and



05-4506832 🚱 pustaka.upsi.edu.my 🚹 Perpustakaan Tuanku Bainun 💟 PustakaTBainun 👘 ptbupsi



#### Perpustakaan Tuanku Bainun Kampus Sultan Abdul Jalil Shah

PustakaTBain

ptbups

2

small scale vortices (Choi and Lee, 2009; Glezer and Coles, 1990; Liu, Dey, Boss, Marquet, and Javidi, 2011; Von Ellenrieder, Kostas, and Soria, 2001; Westerweel, Elsinga, and Adrian, 2013; Zhang, Tao, and Katz, 1997).

There are several flow measurement techniques commonly used and commercially available. These include hot wire anemometry (HWA), laser Doppler anemometry (LDA), particle image velocimetry (PIV), and holographic particle image velocimetry (HPIV). Both hot wire anemometry and laser Doppler anemometry are established point measurement technique where the latter is more favorable since it is a non-intrusive optical measuring technique. Meanwhile, particle image velocimetry in its original form is limited to in-plane two-dimensional two-component (2D-2C) displacement and velocity measurements. Although it is possible to extract the out-of-plane component through stereoscopic viewing (2D-3C), the useful measurement volume remains limited to a light sheet of several millimeters thick. On the other hand, integration of holography in the particle image velocimetry technique finally realised whole-field, three-dimensional three-component (3D-3C) has displacement and velocity measurements (Hinsch, 2002). In brief, holography was invented by Gabor to correct for the spherical aberration of the electron lenses by means of two-step imaging process: (a) recording and (b) reconstruction steps (Gabor, 1948; Gabor, 1949).



05-4506832

Perpustakaan Tuanku Bainun Kampus Sultan Abdul Jalil Shah

PustakaTBainur

O ptbu

3

Holographic particle image velocimetry is a promising technique to probe and characterize complex flow dynamics (Hinsch, 2002; Katz and Sheng, 2010). It simply records the coherent light scattered by small seeding particles (several micrometres in diameter) that are assumed to faithfully follow the flow and uses it to reconstruct the event afterward. A hologram records objects in the form of complex interference fringes and contains useful amplitude and phase information that provide the means to make three-dimensional three-component measurements. Displacement (or velocity) of particle images can be extracted by focusing the images using a travelling video microscope. Due to cumbersome chemical processing associated with holographic films as recording medium, attention of the fluid community has shifted to using CCD sensors. This offers enormous advantages since digital hologram of particle images of can be analysed numerically. As a result, 3D flow measurement technique using holography eventually has emerged in the form of digital HPIV (DHPIV) and micro-digital HPIV (µDHPIV) techniques.

#### **1.2 Problem Statement**

Characterization of both large and small scale vortices is directly related to spatial resolution which in turn depends on concentration of the seeding particles. Although it is desirable to seed the flow under investigation with a relatively high particle concentration for more precise characterization, this consequently results in the

Perpustakaan Tuanku Bainun Kampus Sultan Abdul Jalil Shah



PustakaTBainu

ptbups

4

increase of noise contributed by out-of-focus particle images. This type of noise increases with the increase of particle concentration (Katz and Sheng, 2010; Royer, 1974; Sheng, Malkiel, and Katz, 2006), causing problems especially in (a) differentiating between noise and particle image, and (b) unintentionally masking neighbouring particles that lie above and below, in which the mask is applied to avoid detecting the same particle twice. It is noted that this particular noise remains exist even though the employed optical imaging system is ideally free from other physical noise.

Another dominant problem that exists in these three aforementioned measurement techniques (HPIV, DHPIV, and µDHPIV) is aberrations. Aberration is obtained as it causes reconstructed particle images to appear in the shape of complex 3D morphology, making identification of particle images difficult and inaccurate determination of particle centroid. Aberration also severely restricts the maximum number of particle images that can be extracted. Sources of aberrations include: (a) experimental apparatus (Verrier, Coëtmellec, Brunel, and Lebrun, 2008; Verrier, Remacha, Brunel, Lebrun, and Coëtmellec, 2010), (b) optical misalignment (Cho, Kim, Yu, Shin, and Jung, 2009; Colomb, Montfort, Kühn, Aspert, Cuche et al., 2006; Zhang et al., 1997), and (c) non-uniform shrinkage of a holographic film (Barnhart, Adrian, and Papen, 1994). For example, often cylindrical channels are utilised in the laboratory setup to simulate actual flow down to the minutest details, however, this causes aberration (for example, astigmatism) in the particle images. In large-scale flow, use of corrective optics was found useful to correct for the distortion

Perpustakaan Tuanku Bainun Kampus Sultan Abdul Jalil Shah

Ő



PustakaTBainu

ptbup

5

introduced by a thick cylindrical window (Alcock, Garner, Halliwell, and Coupland, 2004). Nonetheless, this approach is not foreseen as a practical step in a micro-scale flow.

In comparison to digital techniques (DHPIV and µDHPIV), conventional HPIV recording using holographic films is often subject to aberrations introduced in the reconstruction step. Correction of the aberrations is usually done optically and laboriously time consuming (Hinsch, 2002; Katz and Sheng, 2010), whereby the resulting intensity image is continuously recorded and checked using the travelling video microscope. In this process, the phase information of the reconstructed particle image is completely loss and this is considered as the main drawback. To the best of protoke upsted using the reported holographic reconstruction methods in the literature has managed to record both amplitude and phase simultaneously, limiting the possibility to perform digital aberration correction.

In order to extract as greater number of particle images as possible thereby offering increased spatial resolution, care must be taken to consider the effects of noise and aberration. This thesis deals with the techniques to maximize detection of particle images, automate pattern recognition for image classification and correction of the aberrations in the particle images recorded either using CCD sensors or/and holographic films.

